Power System Network Reduction for Power Hardware-in-the-Loop Simulation

Preprint

Bin Wang, Andy Hoke, and Jin Tan

National Renewable Energy Laboratory

Presented at the 2021 IEEE Kansas Power and Energy Conference (KPEC)
April 19–20, 2021

NREL is a national laboratory of the U.S. Department of Energy
Office of Energy Efficiency & Renewable Energy
Operated by the Alliance for Sustainable Energy, LLC

This report is available at no cost from the National Renewable Energy Laboratory (NREL) at www.nrel.gov/publications.

Contract No. DE-AC36-08GO28308

Conference Paper
NREL/CP-5D00-78372
April 2021

Power System Network Reduction for Power Hardware-in-the-Loop Simulation

Preprint

Bin Wang, Andy Hoke, and Jin Tan

National Renewable Energy Laboratory

Suggested Citation
Wang, Bin, Andy Hoke, and Jin Tan. 2021. *Power System Network Reduction for Power Hardware-in-the-Loop Simulation: Preprint*. Golden, CO: National Renewable Energy Laboratory. NREL/CP-5D00-78372. https://www.nrel.gov/docs/fy21osti/78372.pdf.

NREL is a national laboratory of the U.S. Department of Energy
Office of Energy Efficiency & Renewable Energy
Operated by the Alliance for Sustainable Energy, LLC

This report is available at no cost from the National Renewable Energy Laboratory (NREL) at www.nrel.gov/publications.

Contract No. DE-AC36-08GO28308

Conference Paper
NREL/CP-5D00-78372
April 2021

National Renewable Energy Laboratory
15013 Denver West Parkway
Golden, CO 80401
303-275-3000 • www.nrel.gov

NOTICE

This work was authored in part by the National Renewable Energy Laboratory, operated by Alliance for Sustainable Energy, LLC, for the U.S. Department of Energy (DOE) under Contract No. DE-AC36-08GO28308. Funding provided by the U.S. Department of Energy Office of Energy Efficiency and Renewable Energy Solar Energy Technologies Office Agreement Number 34224. The views expressed herein do not necessarily represent the views of the DOE or the U.S. Government.

Cover Photos by Dennis Schroeder: (clockwise, left to right) NREL 51934, NREL 45897, NREL 42160, NREL 45891, NREL 48097, NREL 46526.

Power System Network Reduction for Power Hardware-in-the-Loop Simulation

Bin Wang, Andy Hoke and Jin Tan
National Renewable Energy Laboratory
Golden, US
{bin.wang, andy.hoke, jin.tan}@nrel.gov

***Abstract*—This paper proposes single-port equivalent and two-port equivalent network reduction methods to respectively reduce single-port and two-port areas in a large power network. Parameters of the reduced systems are rigorously derived, which guarantees that the electrical quantities at the port(s) remain unchanged over the reduction, including voltage magnitude and phase and active and reactive power injections into the area to be reduced. The proposed techniques are applied to reduce a practical Maui grid, where the total numbers of buses, lines and transformers are respectively reduced from 212, 106 and 108 to 45, 30 and 13. Dynamic behaviors between the full model and the reduced model are compared in detail to illustrate the efficacy and accuracy of the proposed network reduction.**

***Index Terms*—Network reduction, single-port equivalent, two-port equivalent, model reduction**

I. Introduction

New system-level dynamic risks have come along with the increased renewable penetration [1] since early 2000, e.g. subsynchronous oscillations. The unavailability of accurate newly added dynamic model elements, like inverter-based generation, electric vehicles, batteries and motors, make it difficult to simulate, analyze and understand the mechanism of and acquire the solution to these new problems, posing a challenge to the ambitious 100%-renewable goal pursued by many states [2].

Power hardware-in-loop (PHIL) testing allows an accurate simulation of systems containing elements with inaccurate or unavailable dynamic models by replacing them with actual hardware connected to the rest of the simulation via an analog-digital interface. Therefore, PHIL can be used to investigate potential detrimental interactions, and de-risk field deployment by pre-testing in a laboratory [3].

PHIL simulation requires that the model run in real time, so conducting PHIL testing for a large system often requires a model reduction [4], including network reduction and dynamic model aggregation, to fit into the capability of available real-time simulation tools. There have been extensive efforts in the past half century on power system model reduction [5]-[11]. To name a few, the earliest technique named Ward equivalent [5] and its variations [6] may not retain power flow patterns over the reduction, and they usually result in a highly dense impedance matrix which may not lead to a better computational efficiency. The Dynamic Reduction Program (DYNRED), originally developed by EPRI in early 1990s [7], was enhanced in 2010 [8] to better fit into online environments. In addition, the network reduction efforts also extend to other advanced techniques [9] [10] like HELM, and to distribution systems [11] targeting radial network typologies.

This paper proposes two new power-flow-preserving network reduction techniques that we believe are easier to implement and more intuitive than existing techniques. More importantly, the software tool based on the proposed idea will be made free and publicly available [12]. The techniques proposed in this paper begin by identifying areas to be reduced, and they can be applied iteratively for different parts of the system in sequence until the desired level of reduction is reached. These techniques allow identification of reducible instances even in meshed networks, where dynamic elements to be tested by PHIL could spread all over the network. The two proposed techniques involve identifying single-port equivalent and two-port equivalent networks for reduction and then applying simple equations to derive the reduced network. These two techniques are based on Kirchhoff's current law and can guarantee that the power flow patterns remain unchanged for the rest of the system over the reduction.

The rest of the paper is organized as follows: Section II derives the reduce techniques. Section IV presents a case study on Maui power grid. Conclusions are drawn in Section V.

II. Single-Port and Two-Port Equivalents

In this section, the single-port and two-port equivalent techniques are proposed for power system network reduction. The key idea is to derive a reduced system that is equivalent to the single-port or two-port area of the original system in terms of the terminal voltage and power injection at the port. A single-port (or two-port) area in a power system is defined as a portion of the system that is connected to the rest of the system through exactly one (or two) ports, where a port is usually a transmission path, as illustrated in figures in the next

This work was authored by the National Renewable Energy Laboratory, operated by Alliance for Sustainable Energy, LLC, for the U.S. Department of Energy (DOE) under Contract No. DE-AC36-08GO28308. This material is based upon work supported by the U.S. Department of Energy's Office of Energy Efficiency and Renewable Energy (EERE) under Solar Energy Technologies Office (SETO) Agreement Number 34224. The views expressed in the article do not necessarily represent the views of the DOE or the U.S. Government. The U.S. Government retains and the publisher, by accepting the article for publication, acknowledges that the U.S. Government retains a nonexclusive, paid-up, irrevocable, worldwide license to publish or reproduce the published form of this work, or allow others to do so, for U.S. Government purposes.

two subsections. The network reduction techniques described here assume that distributed generation in each single-port or two-port area shares common dynamic model, and likewise that loads in each single-port or two-port area share common dynamic models.

A. Single-Port Equivalent

Given a single-port area, as shown in Fig. 1, where there are n loads, denoted as $P_{\mathrm{L}1}$, $Q_{\mathrm{L}1}$, $P_{\mathrm{L}2}$, $Q_{\mathrm{L}2}$, ..., $P_{\mathrm{L}n}$, $Q_{\mathrm{L}n}$, and m distributed generation units (DGs), denoted as $P_{\mathrm{dg}1}$, $Q_{\mathrm{dg}1}$, $P_{\mathrm{dg}2}$, $Q_{\mathrm{dg}2}$, ..., $P_{\mathrm{dg}m}$, $Q_{\mathrm{dg}m}$, which are connected to the root bus through a passive network. Denote voltage magnitudes as $V_{\mathrm{L}1}$, $V_{\mathrm{L}2}$, ..., $V_{\mathrm{L}n}$, $V_{\mathrm{dg}1}$, $V_{\mathrm{dg}2}$, ..., $V_{\mathrm{dg}m}$ for corresponding load and DG buses, and the power injection from the rest of the grid as P_{in} and Q_{in} at the root bus, whose voltage is $V\angle\theta$. If the single-port area injects active or reactive power, P_{in} or Q_{in} is negative. Note that all powers and voltages are in pu. Note that all power and voltage quantities are in pu.

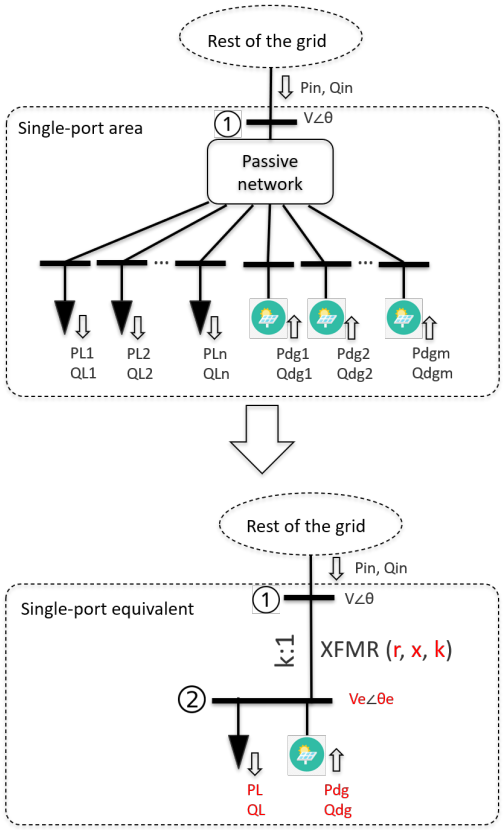

Fig. 1. Reduction of a single-port area to derive an equivalent single-port network.

Assume that the single-port area can be reduced to a single-port equivalent system as shown in Fig. 1 with 9 real-valued unknowns in red color, where the voltage at bus 2 is $V_{\mathrm{e}}\angle\theta_{\mathrm{e}}$; the resistance, reactance and turns ratio of branch 1-2 are r, x and k; and the equivalent power of load and DG are P_{L}, Q_{L}, P_{dg} and Q_{dg}. Applying Kirchhoff's current law (KCL) respectively at bus 1 and bus 2 in the reduced system gives 2 complex-valued equations (1)-(2), leading to only 4 real-valued equations that cannot solve for 9 unknowns.

$$\left(\frac{P_{\mathrm{in}}+jQ_{\mathrm{in}}}{V\angle\theta}\right)^{*}=\frac{V\angle\theta}{r+jx}-\frac{V_{\mathrm{e}}\angle\theta_{\mathrm{e}}}{k(r+jx)} \tag{1}$$

$$\frac{-V\angle\theta}{k(r+jx)}+\frac{V_{\mathrm{e}}\angle\theta_{\mathrm{e}}}{k^2(r+jx)}=\left(\frac{P_{\mathrm{dg}}-P_{\mathrm{L}}+j(Q_{\mathrm{dg}}-Q_{\mathrm{L}})}{V_{\mathrm{e}}\angle\theta_{\mathrm{e}}}\right)^{*} \tag{2}$$

To make the problem solvable, it is assumed that the following equations (3)-(5) hold. The following are a few explanations to justify the five equations (3)-(5): (i) eq. (3) guarantees the total load in the single-port area is equal to that of the reduced system; (ii) eqs. (4) guarantees the conservation of total DG active and reactive power; and (iii) eq. (5) means that the voltage magnitude of bus 2 in the reduced system is defined as the average voltage of all load and DG buses in the original single-port area.

Then, with eqs. (1)-(5), r, x, k and θ_{e} can be uniquely solved: (i) taking the magnitude of the complex-valued equation $k\times$(1)+(2) results in a real-valued equation with only one unknown k, therefore, k is solved as shown in (6); (ii) similarly, taking the angle of the complex-valued equations in (i) can lead to the solution θ_{e} in (8); substituting k and θ_{e} into eq. (1) gives the solution to r and x.

$$P_{\mathrm{L}}=\sum_{i=1}^{n}P_{\mathrm{L}i},\quad Q_{\mathrm{L}}=\sum_{i=1}^{n}Q_{\mathrm{L}i} \tag{3}$$

$$P_{\mathrm{dg}}=\sum_{i=1}^{m}P_{\mathrm{dg}i},\quad Q_{\mathrm{dg}}=\sum_{i=1}^{m}Q_{\mathrm{dg}i} \tag{4}$$

$$V_{\mathrm{e}}=\frac{1}{n+m}\left(\sum_{i=1}^{n}V_{\mathrm{L}i}+\sum_{i=1}^{m}V_{\mathrm{dg}i}\right) \tag{5}$$

$$k=\frac{V_{\mathrm{e}}}{V}\cdot\frac{\sqrt{P_{\mathrm{in}}^2+Q_{\mathrm{in}}^2}}{\sqrt{(P_{\mathrm{L}}-P_{\mathrm{dg}})^2+(Q_{\mathrm{L}}-Q_{\mathrm{dg}})^2}} \tag{6}$$

$$\alpha=V_{\mathrm{e}}\frac{P_{\mathrm{in}}+jQ_{\mathrm{in}}}{V\angle\theta} \tag{7}$$

$$\theta_{\mathrm{e}}=\sin^{-1}\frac{k(Q_{\mathrm{L}}-Q_{\mathrm{dg}})}{\sqrt{\mathrm{Re}(\alpha)^2+\mathrm{Im}(\alpha)^2}}-\tan^{-1}\frac{\mathrm{Im}(\alpha)}{\mathrm{Re}(\alpha)} \tag{8}$$

$$Z=\frac{V\angle\theta-\frac{V_{\mathrm{e}}}{k}}{\left(\frac{P_{\mathrm{in}}+jQ_{\mathrm{in}}}{V\angle\theta}\right)^{*}} \tag{9}$$

$$r=\mathrm{Re}\{Z\},\quad x=\mathrm{Im}\{Z\} \tag{10}$$

To summarize, the above single-port equivalent maintains the following quantities unchanged over the reduction from the original network: the power injection at the root bus, the magnitude and angle of the root bus, and the total load and total DG in the single-port area.

B. Two-Port Equivalent

The two-port equivalent follows a similar idea, but deals with a two-port area as illustrated in Fig. 2. It is assumed that the two-port area can be reduced to a two-port equivalent with 10 real-valued unknowns in red color in Fig. 2. Applying KCL at buses 1, 2 and 3 can result in 3 complex-valued equations (11)-(13), i.e. 6 real-valued equations that cannot solve 10 unknowns. Several variables in these equations are defined in Fig. 2. Similar to (3)-(4), assuming the conservation of total load and total DG active and reactive powers can eliminate 4 unknowns. Then, the resulting unknowns can be solved from (11)-(13), and their solutions are explicitly shown in (14)-(16).

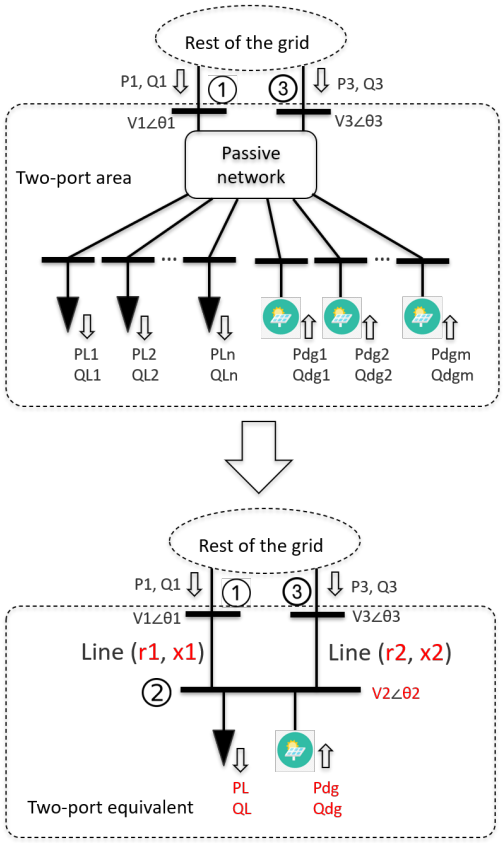

Fig. 2. Reduction of a two-port area to derive an equivalent two-port network.

$$\left(\frac{P_1+jQ_1}{V_1\angle\theta_1}\right)^* = \frac{V_1\angle\theta_1 - V_2\angle\theta_2}{r_1+jx_1} \tag{11}$$

$$\left(\frac{P_{\rm dg}-P_{\rm L}+j(Q_{\rm dg}-Q_{\rm L})}{V_2\angle\theta_2}\right)^* = \frac{V_1\angle\theta_1 - V_2\angle\theta_2}{r_1+jx_1} + \frac{V_3\angle\theta_3 - V_2\angle\theta_2}{r_2+jx_2} \tag{12}$$

$$\left(\frac{P_3+jQ_3}{V_3\angle\theta_3}\right)^* = \frac{V_3\angle\theta_3 - V_2\angle\theta_2}{r_2+jx_2} \tag{13}$$

$$V_2\angle\theta_2 = \frac{P_{\rm dg}-P_{\rm L}+j(Q_{\rm dg}-Q_{\rm L})}{\frac{P_1+jQ_1}{V_1\angle\theta_1}+\frac{P_3+jQ_3}{V_3\angle\theta_3}} \tag{14}$$

$$r_1+jx_1 = \frac{V_1\angle\theta_1 - V_2\angle\theta_2}{\left(\frac{P_1+jQ_1}{V_1\angle\theta_1}\right)^*} \tag{15}$$

$$r_2+jx_2 = \frac{V_3\angle\theta_3 - V_2\angle\theta_2}{\left(\frac{P_3+jQ_3}{V_3\angle\theta_3}\right)^*} \tag{16}$$

C. Remarks

This section has derived reduced systems for single-port and two-port areas in a power grid, which can guarantee (i) the conservation of total load and total DG within the area, and (ii) the equivalence of steady-state terminal quantities, including active and reactive power injections, voltage magnitude and angle. Therefore, when applying these two techniques, the power flow of the rest of the system will remain unchanged. Note that in the reduced model, the voltage(s) and power injections at the ports may change when system loading and/or dispatch are modified.

In deriving the single- and two-port equivalents, two assumptions were implicitly adopted by this section to allow all loads and DGs in the area to be combined by, e.g., scaling MVA and moved to bus 2: (i) all loads and DGs share the same voltage level, and (ii) all loads and all DGs respectively share the common dynamic models. However, these assumptions are usually not perfectly satisfied in practice. In fact, a slight modification to the proposed techniques could address these issues. The idea is to select the voltage level associated with majority of the loads and DGs in the area for bus 2. Then, each of the elements with a different either voltage level or dynamic model can be then connected to bus 2 through a zero-impedance transformer, as illustrated in Fig. 3.

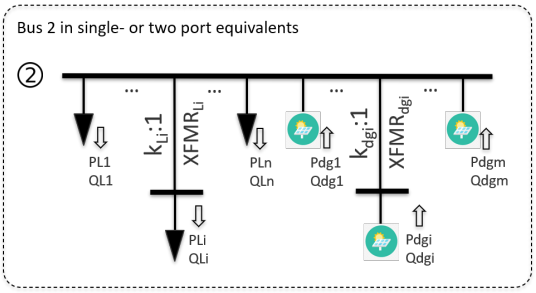

Fig. 3. Connection to bus 2 through zero-impedance transformer.

Still, it should be noted that the dynamic behavior of the entire system may be altered, to some extent, over the reduction, since the electric connection within the reduced area is changed. It will be shown in the next section by testing a real power grid that the loss of accuracy could be very little in the system dynamics.

III. NETWORK REDUCTION OF MAUI GRID

A. Maui Grid

The state of Hawaii historically relied heavily on imported petroleum and coal for power, due to its isolated location and lack of fossil fuel resources, and as of 2016 its electricity

prices were about 2-3 times the US average [13]. With its consistently decreasing costs, renewable energy generation in Hawaii has been drastically increased in the last decade [14]. The second largest island in Hawaii, Maui island, as shown in Fig. 4, has a total renewable energy installation of about 190MW, including over 100MW distributed generation and 72MW wind, plus 75MW hybrid power plants (PV+battery) in development [15].

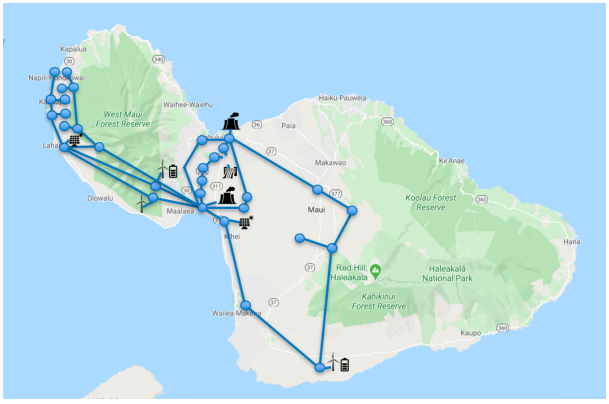

Fig. 4. Maui island and the one-line diagram of its 69kV transmission system.

A day minimum PSS/E case of the Maui grid was provided by Hawaii Electric Company (HECO), which has a very high instantaneous renewable penetration level of 82.9%. A summary of the system's basic information is provided in Table I.

TABLE I
BASIC INFORMATION ABOUT HECO DAY MINIMUM CASE

Total load	162.0 MW	Distributed PV	67.0 MW
Total generation	164.0 MW	Utility-scale PV	5.4 MW
Total renewable	136.0 MW	Wind	63.6 MW
Total inertia	225.3 MVA·s	Min voltage level	0.48 kV
Renewable penetration	82.9%	Max voltage level	69 kV

B. Network Reduction

After ten single-port areas and six two-port areas are respectively identified and then reduced by the proposed techniques, along with combining lines in parallel and in series, the Maui grid can be reduced into a much smaller system, as summarized in Table II. More details are listed below.

- *Synchronous generator*: Four small behind-the-meter hydro units, rating from 1.35MW to 1.67MW, were combined into one equivalent hydro unit, while the remaining five thermal units remained unchanged.
- *Distributed PV*: There are three types of distributed PV, differing from each other in the frequency tripping characteristics, while all are dynamically represented by the first-generation renewable model. As a matter of fact, all distributed PVs of the same type share the same frequency tripping characteristics. Therefore, distributed PVs from different voltage levels were directly combined via the proposed techniques. The resulting 36 PVs are connected to 12 buses in the reduced system, where each bus has three PVs of different types.
- *Load*: Loads from different voltage levels were directly combined in terms of MW, Mvar and settings of under-frequency load shedding. This is achievable since, in the full PSS/E model, loads are represented by constant current for MW portion and by constant impedance for Mvar portion.

TABLE II
SUMMARY OF MAUI GRID NETWORK REDUCTION

Elements	# in full model	# in reduced model
Synchronous generator	9	6
Bus	212	45
Line	106	31
Transformer	108	13
Load	89	13
Distributed PV	171	36
Utility-scale PV	2	2
Wind	4	4
Battery	1	1

C. Validation of Reduced Maui Grid

To validate the reduced Maui grid, a dynamic simulation is conducted in PSS/E subject to a large disturbance, and compared with the result on the full Maui model. A three-phase fault (fault resistance = 1.5 Ohm) is added to a 69 kV bus near Maalaea power plant at $t = 1.0$ s, and cleared in 5 cycles, where thermal unit M16 is tripped upon the fault clearance. The simulation lasts for 15 seconds. The detailed sequence of events is listed below.

- At $t = 1.0$s, three-phase fault added.
- $t = 1.0833$s, fault cleared and 9MW generation at M16 tripped.
- At $t = 1.24$s, system frequency reached 59.29Hz. Under frequency protection timer of all distributed PVs of one type started, since their first pick-up frequency is 59.3Hz.
- At $t = 1.4$s, all 3.4MW distributed PVs of that type tripped.

Fig. 5-11 show detailed comparisons (including one plot in frequency-domain in Fig. 8) of all generations and loads between the full Maui model and the reduced model, while Table III summarizes the errors in system response; the largest errors always occur during transients. A good match can be observed in steady-state, dynamic, and frequency-domain responses of the system, which demonstrates the validity of the proposed network reduction techniques.

TABLE III
MEAN AND STD DEV OF ERRORS IN THE RESPONSE OF REDUCED MODEL

	V at faulted bus	Hz at faulted bus	MW generation[a]
Mean	0.0029 pu	9.0×10^{-4} Hz	0.71 MW
Std Dev	0.0030 pu	0.013 Hz	0.65 MW

[a] Largest mean and std dev of errors among all generating units.

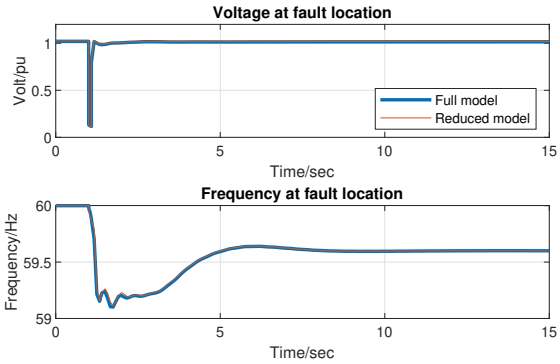

Fig. 5. Voltage and frequency of the faulty bus.

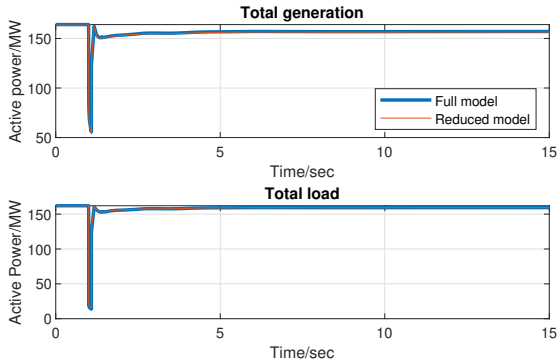

Fig. 6. Total generation and total load.

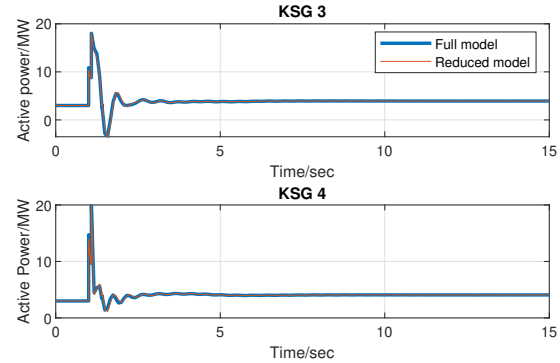

Fig. 7. Kahului generation.

IV. Conclusions and Future Work

This paper proposes two new network reduction techniques based on Kirchhoff's current law, namely single-port equivalent and two-port equivalent. Parameters in the reduced system are determined by fixing the voltage and power at the port, such that the power flow pattern of the rest of the system remains unchanged over the reduction. A case study conducted on a real utility power network model demonstrates the accuracy and effectiveness of the proposed network reduction techniques.

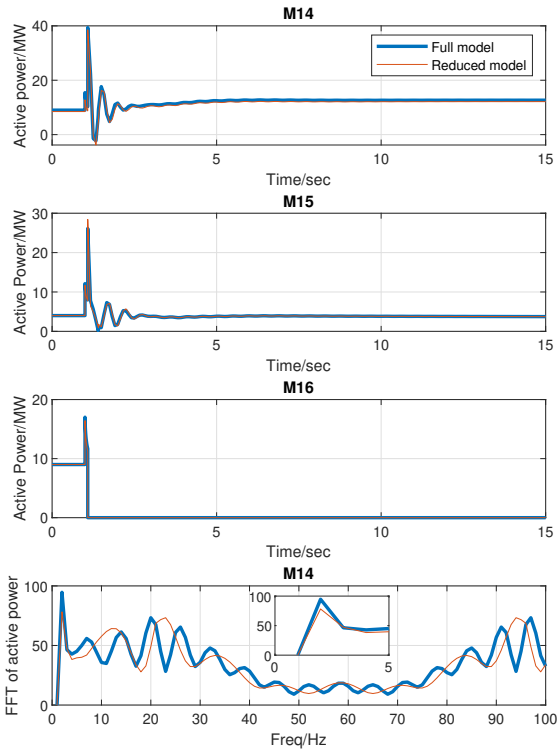

Fig. 8. Maalaea synchronous generation. The top three figures show time-domain comparisons, and the bottom figure shows a frequency-domain comparisons.

Future works include comparisons with other methods, e.g. Ward [5] and HELM [9] based reductions.

Acknowledgment

The authors thank Chris Antonio, Gemini Yau and Marc Asano from Hawaii Electric Company, Inc., and Harry Yuan and Jing Wang from NREL for helpful discussions.

References

[1] L. Zhang, B. Wang, X. Zheng, W. Shi, P. R. Kumar, and L. Xie, "A hierarchical low-rank approximation based network solver for emt simulation," *IEEE Transactions on Power Delivery*, pp. 1–1, 2020.
[2] Environment America, "100% renewable," 2020.
[3] RTDS Technologies, "Power hardware in the loop simulation," 2018.
[4] Andy Hoke, Austin Nelson, Jin Tan, et al, "The frequency-watt function simulation and testing for the hawaiian electric companies," 2017.
[5] J. B. Ward, "Equivalent circuits for power-flow studies," *Trans. of the AIEE*, vol. 68, no. 1, pp. 373–382, 1949.
[6] S. Deckmann, A. Pizzolante, A. Monticelli, B. Stott, and O. Alsac, "Studies on power system load flow equivalencing," *IEEE Trans. on Power Apparatus and Systems*, vol. PAS-99, no. 6, pp. 2301–2310, 1980.
[7] P. Kundur, G. J. Rogers, D. Y. Wong, J. Ottevangers, and L. Wang, "Dynamic reduction," *EPRI TR-102234 Project 244701*, 1993.
[8] L. Wang and G. Zhang, "Dynred enhancement project," *EPRI TR for Software Product ID 1020268*, 2010.
[9] Y. Zhu, D. Tylavsky, and S. Rao, "Nonlinear structure-preserving network reduction using holomorphic embedding," *IEEE Transactions on Power Systems*, vol. 33, no. 2, pp. 1926–1935, 2018.

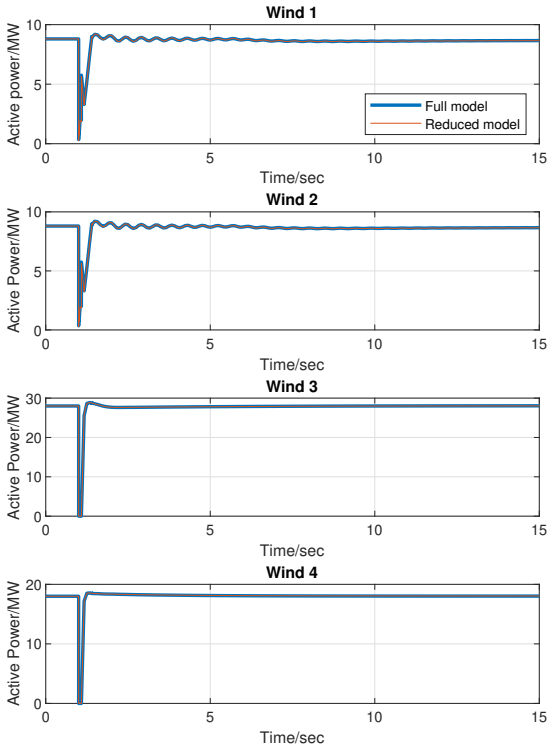

Fig. 9. Wind generation.

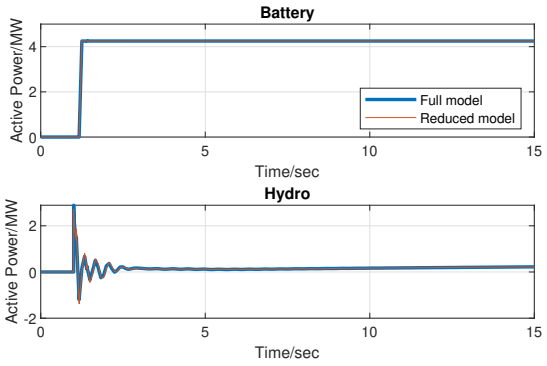

Fig. 10. Battery output and hydro generation.

[10] Q. Ploussard, L. Olmos, and A. Ramos, "An efficient network reduction method for transmission expansion planning using multicut problem and kron reduction," *IEEE Transactions on Power Systems*, vol. 33, no. 6, pp. 6120–6130, 2018.

[11] A. Nagarajan, A. Nelson, K. Prabakar, A. Hoke, M. Asano, R. Ueda, and S. Nepal, "Network reduction algorithm for developing distribution feeders for real-time simulators," in *2017 IEEE Power Energy Society General Meeting*, pp. 1–5, 2017.

[12] NREL, "PSSE Network Reduction." [Accessed: 2021-03-30] https://github.com/NREL/PSSE_Network_Reduction.

[13] U.S. Energy Information Administration, "Table 5.6.a. average price of electricity to ultimate customers by end-use sector, by state, august 2020 and 2019," 2020.

[14] Hawaii State Energy Office, "Hawaii energy facts & figures," 2019.

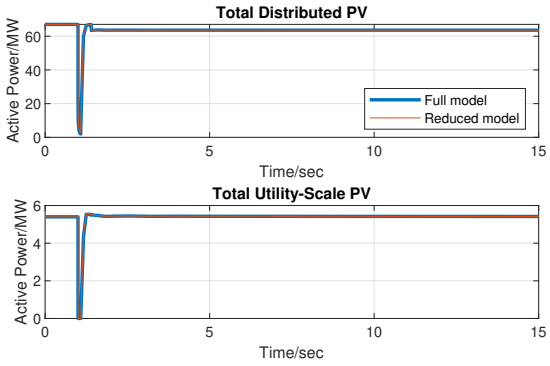

Fig. 11. Distributed and utility-scale PV.

[15] Hawaii Electric Company, Inc., "Power facts," 2020.